Pseudoelasticity on low carbon steel

M. Notomi[1]

Summary

The deformation behaviors of low carbon steels exposed to several heat treatment conditions are studied with the optical microscopic observation. The quenched specimens possess martensite texture exhibit pseudoelasticity during the cyclic tensile loading tests. The specimens as-received and annealed at the higher temperatures possess ferrite and pearlite textures exhibit plasticity. The specimens tempered after quenched possess martensite texture and annealed at the lower temperatures exhibit plasticity firstly and then pseudoelasticity.

Introduction

In 1971 Nagasawa found that a Fe-based alloy, Fe-Ni exhibits slight shape memory effect [1]. The effect of 304 type stainless steel was found in 1971 by Enami et al [2]. The authors reviewed crystallographic and physical properties of the binary shape memory alloys [3] at 2005. So far it is known that the several kinds of Fe-based alloys, Fe-Mn, Fe-Ni, Fe-Pd, Fe_3Pt and so on. Especially, Fe_3Al single crystals with $D0_3$ structure exhibited the shape memory and the pesudoelasticity effects nevertheless this alloy exhibit no martensitic transformation [4]. It is indicated that the behavior of pesudoelasticity with Fe_3Al was based on the motion of 1/4<111> superpartial dislocations, not stress induced martensitic transformation (MT).

The mechanics of stress induced MT is discussed on the basis of the twinning deformation [5]. A twinning deformation on steel can occur in very low temperature atmosphere and/or with impact loading. If the deformation on steel transit from slipping to twining, the steel might exhibit shape memory effect and/or pesudoelasticity. We conducted cyclic tensile tests for low carbon steel exposed with several kinds of heat treatment and found the pesudoelasticity that is unknown behaviors so far.

Materials and Experiments

Table 1 shows chemical compositions of the material measured by a X-ray fluorescence spectrometer (Rigaku RIX3100) and a carbon/sulfur analyzers (Horiba EMIA-720). The material is steel containing 0.2wt% C and so hypoeutectoid alloy. Dumbbell type specimens with 9 mm diameter are cut from a bar with 13.5mm made of the material. A group of the specimens were

[1] Professor, Meiji University, Japan

conducted the tests without any heat treatment, called as-received. The rest specimens are experienced the four kinds of heat treatments, shown in Table 2, quenching, tempering after quenching and annealing at two different temperatures. In each condition, a specimen was broken by tensile load using a testing machine (MTS 800) and obtained stress-strain relation. Another specimens were applied to specific tensile strain under just yielding and then removed for the stress to zero, that is first cycle. Continuously the specimen was applied again to more strain than the final one of the first cycle and then removed, that is second cycle. The specimens were loaded fourth or fifth cycle due to the failure strain determined by the fracture test. The tests were performed at a constant strain rate of 0.1 mm/s and room temperature. Microstructures on cross-section of the specimens were observed by optical microscopy.

Table 1 Chemical compositions.

C	Si	Mn	Ni	Cr	Mo	Cu
0.2	0.31	0.78	0.06	0.12	<0.05	0.14

[wt%]

Table 2 Heat treatment conditions.

Conditions	Quenching	Tempering	Annealing at High Temp.	Annealing at Low Temp.
Temperature [K]	1173	873	1173	673
Time [sec]	3600	3600	3600	1200
Cooling medium	Water	Water	Air	Air

Failure and Cyclic Loading Tests

The result of the specimen as received with d=9mm until fracture is shown the top in Fig. 1(a). The applying stress decreases with the increase of strain after yielding on which the stress is about 700MPa and then the specimen breaks at 0.15 strains. Fig.1(a) also shows the stress-strain curves of first to fourth cycles. In the first cycle the stress decreases for zero just after the start of unloading and certain strain remains at the zero stress. The second and third cycles are similar to the first one. Consequently, the specimen as-received deforms plastically during these cycles.

The stress-strain relation of the specimen quenched shown in Fig.1(b) exhibits the plateau stress region, about 700MPa, after yielding. Beyond about 0.35 strains the stress increases for attaining the maximum, i.e., work-hardening effect and then it decreases until breaking. The lower figures in Fig.1(b) show the stress-strain relations of first to fourth cycles. In the first cycle the stress increases with the increase the strain and then keeps constant after the stress attains about 700MPa. Just unloading the stress decreases a little and then keeps constant even though the deformed strain recovers. The unloading path of the relation follows about the loading one until the stress to zero. In the second and third cycle, the plateau stress region and strain recovery are also observed as the

almost same as the first one. In the fourth cycle the stress increase beyond the stress plateau region, about 0.38 strains. However, the strain elastically recovers during unloading, that is the specimens as quenched exhibit pseudoelasticity.

Fig. 1(c) shows the stress-strain relations of the tempered specimen. Although the stress plateau region is identified on the stress-strain curve in the failure test, the behavior is different from that of the quenched. The deformation mode of first and second cycles is plastic and residual strains remain at removing the stress. However, during the process of unloading in the third cycle the stress keep the constant and the unloading pass followed the almost loading. It means the deformation mode varies from plastic to pseudo-elastic one. Although the fourth and fifth cycles exhibit pseudo-elastic deformation, some residual strains remain at removing the load. The stress-strain relations of the specimens annealed at 1173K and 673K are shown in Figs. 1(d) and 1(e), respectively. The mode of the specimen annealed at 1173K exhibits plastic deformation, is different from that annealed at 673K, pseudo-elastic one.

Since testing machine errors, e.g. loosing the attachment to specimen, might affect stress-strain relation on cyclic loading tests more than on monotonic ones, the pseudo-elastic behavior has been checked by other measures. The shape recovery that is defined as the ratio of a recovery elongation (= a maximum applied displacement – a residual elongation before and after test) to a maximum applied displacement is obtained from the direct specimen length measurement by a caliper without the output of the testing machine and is show in Table 3. The results also exhibit the recovery, i.e., pseudoelasticity of the quenched and tempered specimens.

Table 3 specimen length changes before and after the cyclic tests.

Heat treatment	Specimen length before test [mm]	Specimen length after test [mm]	Max. applied displacement [mm]	Final shape recovery [%]
Quenching	190.2	190.7	18.0	97.2
Tempering	190.6	195.6	22.5	77.8
Annealing at high T	190.1	198.0	9.0	12.2
Annealing at low T	189.4	191.2	5.0	65.1

Microstructures Observations

Optical micrographs of the specimens as-received, quenched and annealed at 1173K are presented in Fig. 2. The microstructure of the specimen as-received, Fig.2(I), consists of two microconstituent, proecutectoid ferrite and pearlite. Almost of the microstructures on Fig.2 (II) are the needle-shaped grains that are martensite due to quenching. Although an appearance of the specimen as tempered after quenching, the microstructure is similar to that of the quenched specimen, some white regions to be identified as ferrite exist between the phases of martensite. On the other hand the microstructures of the specimen annealed at 1173K in Fig.2(III) and 673K appear ferrite and pearlite like Fig.2(I). The grain

sizes of proeutectoid α (ferrite) on the specimen as annealed at 1173K are larger than that at 673K.

Discussions

The relationship between the deformation modes and the microstructures is considered. Table 4 shows the deformation modes of each cycle and heat treatment condition and the microstructures. The specimens as received and annealed at high temperature exhibit the plastic deformation during all the cycles and have ferrite and pearlite phase. The quenched specimens having typical martensite phase exhibit pseudoelasticity. Moreover, the tempered specimens exhibit the normal plastic deformation until the first two cycles and then pseudoelasticity during the last three cycles even though the optical micrograph shows almost the same martensite phase as the quenched ones. The specimens annealed at lower temperature exhibit the almost same behaviors as that of the tempered specimens although the microstructure has the same as that of the ones annealed at higher temperature, ferrite and pearlite phases. Consequently the

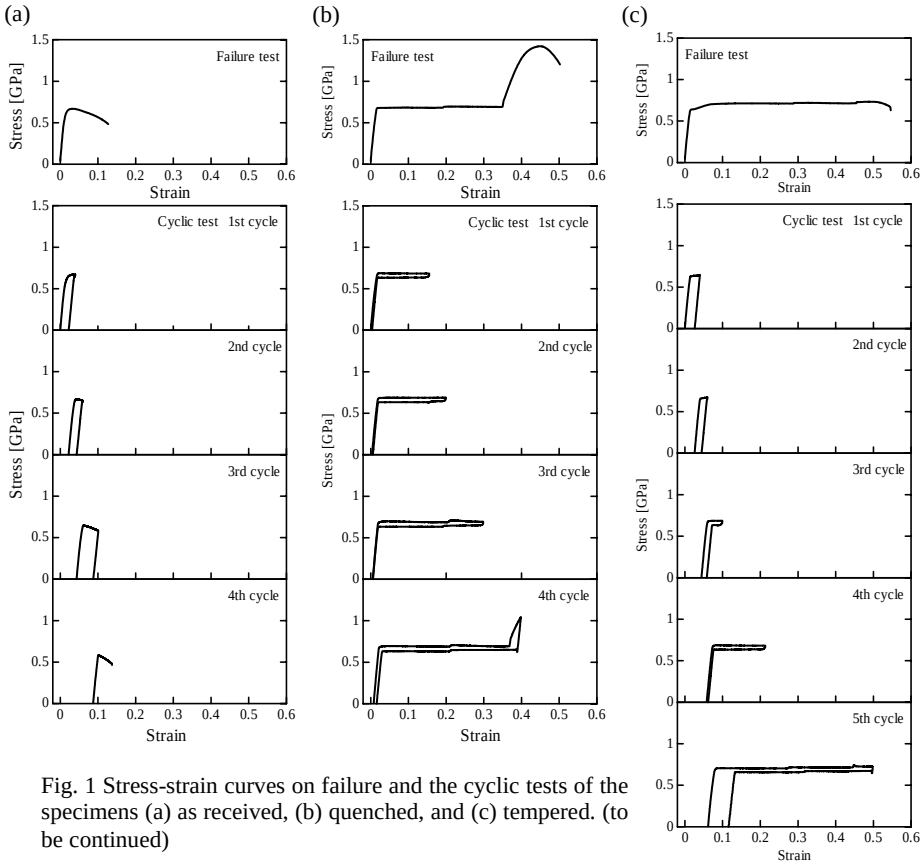

Fig. 1 Stress-strain curves on failure and the cyclic tests of the specimens (a) as received, (b) quenched, and (c) tempered. (to be continued)

martensite phase is a sufficient condition of pseudoelasticity besides not a requirement one.

There are three mechanisms related to the large deformation in crystals: slip, deformation twinning, and shear transformations [6]. The large deformation mode of crystals in the martensite is the deformation twinning that is detwinning, martensite variant rearrangement. This mechanism causes the pseudoelasticity of the quenched and tempered specimens. Of the tempered specimens plastic deformation in the ferrite phase might occur in the first two cycles and then pseudo-elastic one might occur in the martensite phase since the previous plastic deformation is suppressed by work hardening effect. On the other hand a mechanism of the pseudoelasticity on the specimens annealed at lower temperature is also deformation twinning and not shear transformations like the pseudoelasticity at austenite phase of Ti-Ni shape memory alloys. The reason is

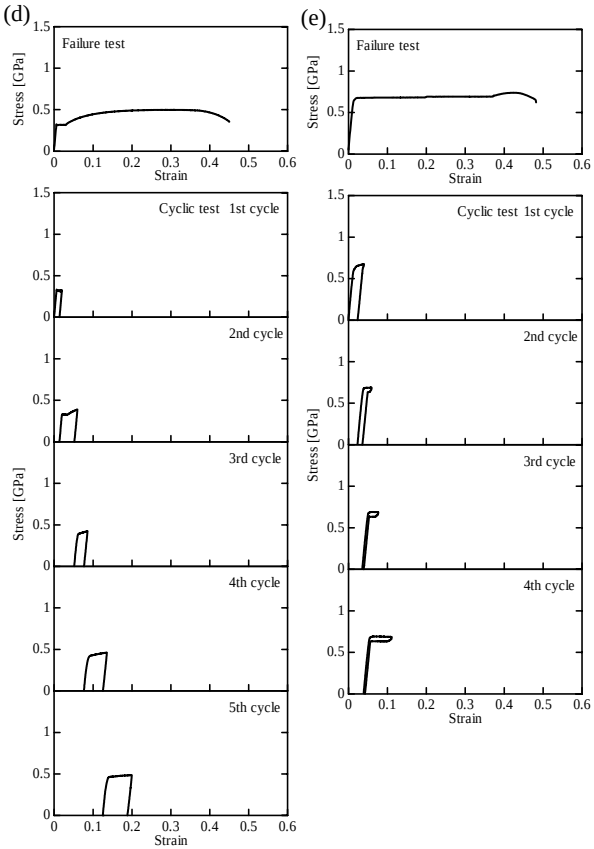

Fig. 1(continued) Stress-strain curves on failure and the cyclic tests of the specimens (d) annealed at 1173K, and (e) annealed at 673K.

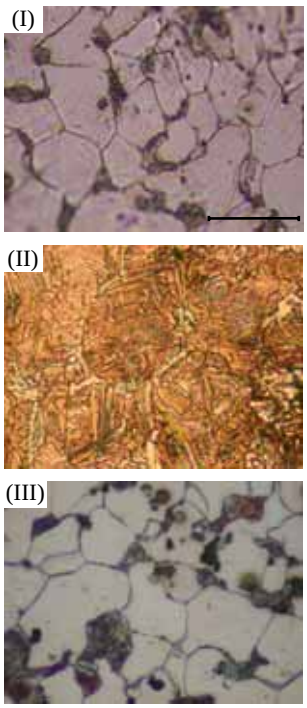

Fig. 2 Optical photomicrographs (I) as received, (II) quenched, (III) annealed at 1173K.

that the ferrite and the cementite could not transform the martensite with diffusionless. In addition to the deformation twinning of pure iron and low carbon steels were observed, while that of high carbon steel were not due to the presence of hard cementite particles [7]. Commonly it is considered that the twin formation in steels occurs most readily under high strain rate and/or low-temperature test conditions [8]. However, it is insisted on that the deformation twinning probably occurs under the testing condition at room temperature with normal strain rate and no one can find a trace of the deformation after tests because of strain recovery due to pseudoelasticity. More investigation will be needed for getting a evidence occurring the twinning deformation and revealing the critical condition for the deformation twinning.

Table 3 Shape recovery determined by specimen length.

Heat treatment	Specimen length before test [mm]	Specimen length after test [mm]	Max. applied displacement [mm]	Final shape recovery [%]
Quenching	190.2	190.7	18.0	97.2
Tempering	190.6	195.6	22.5	77.8
Annealing at 1173K	190.1	198.0	9.0	12.2
Annealing at 673K	189.4	191.2	5.0	65.1

Conclusion

The quenched low carbon steels deformed until large strain occur shape recovery, *i.e*., pseudoelasticity, though the specimens as received exhibit normal plastic deformation. The specimens tempered and annealed at 673K exhibit pseudoelasticity after several loading cycles. The specimens annealed at 1173K only appear the plastic behaviors. The deformation twinning in martensite phases causes to this behavior of the quenched and tempered specimens. Besides, the deformation twinning in ferrite phases probably cause to this of the annealed specimens.

Reference

1 A. Nagasawa, *Physica status solidi, Applied research*, A8 (1971) 531-538.
2 K. Enami, S. Nenno, Y. Minato, *Scripta metallurgica*, 5 (1971) 663-668.
3 M. Notomi, K.J. Van Vliet, S. Yip, *Advanced Intermetallic-Based Alloys*, MRS Proc. 980 (2007) 223-228.
4 H.Y. Yasuda, T. Nakajima, Y. Umakoshi, *Scripta materialia*,55 (2006) 859-862.
5 K. Otuka, C.M. Wayman, in *Shape Memory Materials*, ed. K. Otuka, C.M. Wayman, Cambridge University Press (1998) 11.
6 Alan Cottrell, *An Introduction to Metallurgy* 2nd ed. (1975) 264-266.
7 H.G. Bowden, P.M. Kelly, Deformation twinning in shock-loaded pearlite, *Acta Metallurgica*, Vol.15, (1967) 105-111.
8 Richard W. Hertzberg, *Deformation and Fracture Mechanics of Engineering Materials* (1996) 105-116, John Wiley & Sons, Inc.